Pergamon

0301-9322(94)00063-8

Int. J. Multiphase Flow Vol. 21, No. 2, pp. 267–284, 1995

0301-9322/95 $9.50 + 0.00

ON THE MODELING AND INVESTIGATION OF POLYDISPERSED ROTATING SUSPENSIONS

M. UNGARISH
Department of Computer Science, Technion, Haifa 32000, Israel

(Received 26 April 1994; in revised form 10 August 1994)

Abstract—The flow field associated with the centrifugal separation of non-colloidal polydispersed (in particular, bidispersed) suspensions is considered. The "mixture" model framework is developed, and some indicative solutions are obtained and discussed. It is shown that the treatment of rotating polydispersions, in particular for non-small values of particle Taylor number, encounters idiosyncratic physical and mathematical complications. Therefore, the state of knowledge in the centrifugal case lags much behind the gravity analog.

Key Words: centrifugal separation, polydisperse suspension, bidisperse suspension, two-phase flow, mixture model, diffusion model

1. INTRODUCTION

We consider the *centrifugal separation* of a non-colloidal suspension. The obvious analog is the *gravity settling* process.

Much progress has been made in the last 15 years in the understanding of flow of suspensions in the gravity field, and many of these novel advances have counterpart studies for the centrifugal forcing. However, the almost parallel recent development of knowledge on gravity and centrifugally driven flow of suspensions concerns only monodispersed particles (see Ungarish 1993, where pertinent references are given).

As to polydispersions—i.e. suspensions of particles which differ significantly in size or density—there still are major gaps of knowledge between gravity and centrifugal configurations. To emphasize this gap, we briefly list some fundamental closely-investigated (both experimentally and theoretically) systems of polydispersions in the gravity field:

(1) Straight container, suspension of particles of different densities and/or sizes with a total volume fraction $\varepsilon < 0.16$ (Smith 1966; Greenspan & Ungarish 1982 and others). In this case distinct sectors of smooth one-dimensional flow appear; in each sector the volume fractions ε_j are constant. The theory is simple, straightforward and powerful.
(2) Straight container, mixture of light and heavy particles with $\varepsilon > 0.16$ (approximately) (Fessas & Weiland 1984; Batchelor & Van Rensburg 1986 and others). In this case a strong instability appears in the initial stage, which causes clear fingering and lateral segregation.
(3) Straight container, particles of the same density ρ_D but different sizes suspended in a fluid of density ρ_C, $\varepsilon < 0.16$, and the suspension is overlain by a clear fluid whose density is ρ_U, so that $\rho_D > \rho_U > \rho_C$ (Huppert *et al.* 1991). In this case the flow is one-dimensional, like in the basic configuration (1), but the sharp upper interface descends faster than in the absence of ρ_U layer.
(4) Inclined container, suspension with $\varepsilon < 0.16$ (Davis *et al.* 1982; Schaflinger 1985; Law *et al.* 1988 and others). The flow is smooth and displays distinct zones with clear interfaces between them; extensions of the PNK theory were obtained.

On the other hand, the corresponding state of the art in rotating polydispersions is deficient: to the best of our knowledge, there is only one published work on rotating polydispersions, a theoretical investigation by Ungarish & Greenspan (1984). The analysis considered the (infinitely)

"long" rotating cylinder, in which a suspension of particles of the same density but two different sizes separates from an initial state of solid-body rotation. The solution was obtained via the "two-fluid" model, with drag and effective viscosity assumed to be of Stokesian type.

It is well known that the flow field of a suspension under centrifugal separation is more complex than in gravity settling, mainly because: (a) the force field is space dependent therefore ε must change with time (the "squeezing effect"); and (b) Coriolis accelerations introduce special and counterintuitive effects. The abovementioned analysis points out that when polydispersions are concerned some additional intrinsic differences between the centrifugal and gravity cases appear, which complicate the analysis in the former one, in particular:

- The volume fraction in the left-behind monodispersed mixture sector is both time and space dependent. Therefore, the analytical treatments and relevant experimentation are bound to be difficult.
- The behavior expected due to the gravity-based "intuition" may change drastically when the Taylor numbers of the particles, β_j, are not small. In particular, larger particles may settle slower than the smaller ones. There is presently no direct experimental verification of this trend. The reliability of the formulation for larger β is problematic.

The results of Ungarish & Greenspan (1984) can be viewed as the beginning of the centrifugal counterpart of the basic gravity configuration (1). However, for more complicated cases (i.e. finite cylinder, more components, numerical simulation, stability analysis, spin-up features) it seems necesary to use the more straightforward "mixture model" formulation. The present work, following some preliminary promising results in a simpler configuration (Ungarish 1995), attempts the formulation and solution of polydispersed (in particular, bidispersed) rotating flow problems in the framework of the "mixture model". Essential in this model is the "postulate" for a closure formula for the relative velocities, $\mathbf{v}_{Rj}$, and we shall see that here, again, complications (with no counterparts in gravity) show up. However, under simplifying assumptions a quite straightforward procedure is established and illuminating solutions for centrifugal separation in "long" and finite cylinders are obtained.

2. GOVERNING EQUATIONS

2.1. The main balances

Some essential kinematic relationships between the volume fractions, ε, densities, ρ, velocities, $\mathbf{v}$, and volume flux, $\mathbf{j}$, are given in appendix A. Here we use the "mixture model" formulation. Subscripts D and C denote the dispersed and continuous "phases", mixture variables bear no subscript; $\mathbf{v}_R$ is the relative velocity of phase D measured from phase C. The additional subscript j denotes the particles of type j; this index assumes values 1 and 2 in a bidispersion. For definiteness we denote by 1 the larger and/or heavier particle in the bidispersion. Each component has a constant density, i.e. ρ_C and ρ_{Dj} are constants.

The essential parameters of the flows under consideration are the density coefficient,

$$\epsilon_j = (\rho_{Dj} - \rho_C)/\rho_C, \tag{2.1}$$

and the (modified) Taylor number, which measures the ratio of Coriolis to viscous forces on the dispersed particle,

$$\beta_j = \frac{2}{9}\frac{\Omega}{\nu_0} a_j^2, \tag{2.2}$$

where a is the particle radius, ν_0 is the kinematic viscosity of the pure continuous fluid, and Ω is the angular velocity of the centrifuge. Typically, ϵ_j and β_j are small, but for larger particles in rapid centrifuges non-small values of β_j can appear.

In general, we use a system rotating with constant $\mathbf{\Omega}$ and subject to a constant gravity $\mathbf{g}$. The body force per unit mass is

$$\mathbf{f} = \mathbf{g} - \mathbf{\Omega} \times (\mathbf{\Omega} \times \mathbf{r}) = -\nabla B, \tag{2.3}$$

where

$$B = -\mathbf{g}\cdot\mathbf{r} - \tfrac{1}{2}|\boldsymbol{\Omega}\times\mathbf{r}|^2. \qquad [2.4]$$

In dealing specifically with centrifugal separations we shall use a cylindrical coordinate system r, θ, z where the velocity vector has components u, v, w and $\boldsymbol{\Omega} = \Omega\hat{z}$, and assume that $g \ll \Omega^2 r_o$, where r_o is the outer radius of the container.

The major equations for the mixture fluid are volume continuity,

$$\nabla\cdot\mathbf{j} = 0, \qquad [2.5]$$

and momentum balance

$$\frac{\partial}{\partial t}\rho\mathbf{v} + \nabla\cdot\rho\mathbf{v}\mathbf{v} + 2\boldsymbol{\Omega}\times\mathbf{v} = -\nabla p + (\rho - \rho_C)\mathbf{f} + \nabla\cdot\tau + \nabla\cdot\tau^{\text{diff}}. \qquad [2.6]$$

The continuity ("diffusion") equations for the dispersed phases are

$$\frac{\partial\varepsilon_j}{\partial t} + \nabla\cdot\varepsilon_j\mathbf{v}_{Dj} = 0, \quad j = 1, 2. \qquad [2.7]$$

Here p is the reduced pressure (conventional pressure plus $\rho_C B$), τ is the generalized viscous stress and

$$\tau^{\text{diff}} = -\sum_{j=1}^{2}\varepsilon_j\rho_{Dj}\mathbf{v}_{Rj}\mathbf{v}_{Rj} + \frac{1}{\rho}\left(\sum_{j=1}^{2}\varepsilon_j\rho_{Dj}\mathbf{v}_{Rj}\right)\left(\sum_{j=1}^{2}\varepsilon_j\rho_{Dj}\mathbf{v}_{Rj}\right) \qquad [2.8]$$

is the diffusion stress, see appendix B.

The system [2.5]–[2.8] is supplemented by the kinematic relationships of appendix A. To close it, constitutive relationships for the stress term $\nabla\cdot\tau$ and for the relative velocities, $\mathbf{v}_{R1}$ and $\mathbf{v}_{R2}$, are required. Here we assume that the mixture is Newtonian-like, with a modified, effective viscosity, simply correlated to the viscosity of the pure suspending fluid, as specified later. In the problems we wish to investigate a minor contribution of $\nabla\cdot\tau$ is anticipated, hence the accuracy of that assumption is not critical.

2.2. Relative velocity closure

The closure relationships for $\mathbf{v}_{Rj}$ are essential because the separation process is obviously driven by the interphase relative velocities. In the classic binary gas theory the corresponding closures are provided by Fick's law, but here the "diffusion" (relative motion) of the particles in the embedding fluid is dominated by macroscopic (not molecular) effects.

The task is to model this motion in a simplified manner so that $\mathbf{v}_{Rj}$ (actually, an approximation to it) can be extracted by some elementary manipulations. To this end, it is recalled that in many cases of interest, when the major driving force is the gravity and/or centrifugal buoyancy on the small dispersed particles, the resulting global flow can be considered a small perturbation on some basic, hydrostatic (or geostrophic) inviscid state of the mixture bulk. To be more specific, in such cases, under a relevant scaling which renders the buoyancy term $O(1)$, the Reynolds, the Brownian-diffusion-Peclet and the Grashof numbers are large, and the Rossby number is small, see Ungarish (1993, sections 2.5.4, 2.5.1). Consequently, in the momentum equations the convective accelerations of the particles and mixture and the stresses in the mixture can be assumed much smaller than the buoyancy (body force) terms, which yields the leading balances

$$\rho 2\boldsymbol{\Omega}\times\mathbf{v} = -\nabla p + (\rho - \rho_C)\mathbf{f}; \qquad [2.9]$$

$$\rho_{Dj}2\boldsymbol{\Omega}\times\mathbf{v}_{Dj} = -\nabla p + (\rho_{Dj} - \rho_C)\mathbf{f} + \mathbf{d}_j, \qquad [2.10]$$

where $\mathbf{d}_j$ is the interfacial "drift" (drag plus lift) hydrodynamic force per unit volume on the particle of type j, assumed to be a known function of $\mathbf{v}_{Rj}$. We eliminate the pressure and use [A1]–[A3] to obtain

$$2\boldsymbol{\Omega}\,\frac{\rho_{Dj}\mathbf{v}_{Dj} - \rho\mathbf{v}}{\rho_C} = (c_j - \varepsilon c)\mathbf{f} + \frac{\mathbf{d}_j}{\rho_C}, \qquad [2.11]$$

where, according to the kinematic relationships [A9]–[A10], for $j = 1$,

$$\frac{\rho_{D1}\mathbf{v}_{D1} - \rho\mathbf{v}}{\rho_C} = \frac{1+\epsilon_1}{1+\epsilon\varepsilon}[(1-\varepsilon_1+\epsilon_2\varepsilon_2)\mathbf{v}_{R1} - \varepsilon_2(1+\epsilon_2)\mathbf{v}_{R2}] + (\epsilon_1 - \epsilon\varepsilon)\mathbf{v}, \tag{2.12}$$

and similarly for $j = 2$.

The system [2.11]–[2.12], subject to a given $\mathbf{d}_j = \mathbf{d}_j(\mathbf{v}_{Rj})$, can be used to calculate $\mathbf{v}_{R1}$ and $\mathbf{v}_{R2}$, as follows.

The simplest and widely employed choice for $\mathbf{d}_j$ is the Stokes drag incorporating the effective viscosity correction,

$$\frac{\mathbf{d}_j}{\rho_C} = -\frac{9}{2}\frac{\nu_0}{a_j^2}\mathbf{v}_{Rj}\cdot\mu(\varepsilon), \quad \text{with} \quad \mu(\varepsilon) = \left(1 - \frac{\varepsilon}{\varepsilon_M}\right)^{-2.5\varepsilon_M}; \tag{2.13}$$

see Ishii & Zuber (1979), where ε_M is the maximal packing fraction of the dispersed particles (other similar semi-empirical correlations for $\mu(\varepsilon)$ are often employed).

In pure gravity settling we take $\boldsymbol{\Omega} = 0$ and $\mathbf{f} = \mathbf{g}$; [2.11]–[2.13] readily give

$$\mathbf{v}_{Rj} = \left(\frac{1-\epsilon\varepsilon/\epsilon_j}{\mu(\varepsilon)}\right)\left[\frac{2}{9}\frac{g}{\nu_0}\epsilon_j a_j^2\right]\hat{g}, \tag{2.14}$$

where $\hat{g} = \mathbf{g}/g$. The hindrance function $(1-\varepsilon\epsilon/\epsilon_j)/\mu(\varepsilon)$ reduces to the usual monodispersion form when the particles differ in size but have the same density, $\epsilon_1 = \epsilon_2 = \epsilon$, because in this case the hydrostatic pressure in the mixture depends only on $\varepsilon = \varepsilon_1 + \varepsilon_2$, not on the particular values of ε_1 and ε_2. Equation [2.14] is immediately applicable to more than two dispersed components, e.g. the flow fields calculated by Huppert *et al.* (1991) correspond to [2.14] with $\epsilon = \epsilon_j$ and $\mu(\varepsilon) = (1-\varepsilon)^{-3}$. The closure [2.14] has several convenient features: $\mathbf{v}_{Rj}$ is in the direction of the driving force $\mathbf{g}$; $\mathbf{v}_{R1}$ and $\mathbf{v}_{R2}$ are formally uncoupled; the extension to any number of components is straightforward; $\mathbf{v}_{Rj}$ is space-dependent via ε, and hence consistent with the existence of regions of constant ε_j in the flow-field; in regions of constant ε_j, the term τ^{diff} is also constant (see [2.8]) hence $\nabla\cdot\tau^{\text{diff}}$ vanishes. These properties make [2.14] an extremely facilitating "postulate" for the analysis of polydispersions in the gravity field.

However, in pure centrifugal settling the choice [2.13] leads to less convenient outcomes. One major conceptual difficulty is the applicability of [2.13] in situations where the ratio Coriolis over Stokes forces on the particle is not extremely small, as discussed later. Assuming that [2.13] can be used when $\boldsymbol{\Omega} \neq 0$ and $\mathbf{f} = -\boldsymbol{\Omega}\times(\boldsymbol{\Omega}\times\mathbf{r}) = \Omega^2 r\hat{r}$ we attempt to extract $\mathbf{v}_{R1}$ and $\mathbf{v}_{R2}$ from [2.11]–[2.13]. Recalling the definition [2.2] of the Taylor number of the particle of type j we obtain the two vector equations

$$\mathbf{v}_{Rj} + 2\beta_j\frac{1}{\mu(\varepsilon)}\frac{1+\epsilon_j}{1+\epsilon\varepsilon}\hat{z}\times[\boldsymbol{\alpha}_{jk}\mathbf{v}_{Rj} - \mathbf{c}_k\mathbf{v}_{Rk} + \mathbf{b}_j\mathbf{v}] = \frac{1}{\mu(\varepsilon)}\left(1 - \frac{\varepsilon\epsilon}{\epsilon_j}\right)[\epsilon_j\beta_j\Omega r]\hat{r} \tag{2.15}$$

(for $j = 1$ and $k = 2$, and for $j = 2$ and $k = 1$), where

$$\alpha_{jk} = 1 - \varepsilon_j + \epsilon_k\varepsilon_k; \quad c_k = \varepsilon_k(1+\epsilon_k);$$

$$b_j = \epsilon_j\left(1 - \frac{\varepsilon\epsilon}{\epsilon_j}\right)\frac{1+\epsilon\varepsilon}{1+\epsilon_j}. \tag{2.16}$$

Evidently, for $\beta_j \to 0$ the second term in [2.15] can be neglected and the centrifugal analog of [2.14] follows. Otherwise, the term contributed by the Coriolis acceleration considerably complicates the resulting $\mathbf{v}_{Rj}$, as follows: in addition to the obvious radial component, u_{Rj}, an azimuthal component, v_{Rj}, appears; $\mathbf{v}_{R1}$ and $\mathbf{v}_{R2}$ are directly intercoupled via the c_k terms; $\mathbf{v}_j$ is coupled to the velocity of the embedding fluid, $\mathbf{v}$, via the b_j coefficients.

The scalar equations corresponding to [2.15] are better expressed in dimensionless form upon introducing the scalings

$$L_{\text{ref}} = r_o; \quad V_{\text{ref}} = |\epsilon_1|\beta_1\Omega r_o; \tag{2.17}$$

where r_o is the outer radius of the centrifuge. We obtain

$$\begin{bmatrix} 1 & -2\bar{\beta}_1 & 0 & 2\bar{\beta}_1 A_{12} \\ 2\bar{\beta}_1 & 1 & -2\bar{\beta}_1 A_{12} & 0 \\ 0 & 2\bar{\beta}_2 A_{21} & 1 & -2\bar{\beta}_2 \\ -2\bar{\beta}_2 A_{21} & 0 & 2\bar{\beta}_2 & 1 \end{bmatrix} \begin{bmatrix} u_{R1} \\ v_{R1} \\ u_{R2} \\ v_{R2} \end{bmatrix}$$

$$= \begin{bmatrix} \dfrac{r}{\mu(\varepsilon)}\left(1-\dfrac{\epsilon\varepsilon}{\epsilon_1}\right)\dfrac{\epsilon_1}{|\epsilon_1|} \\ 0 \\ \dfrac{r}{\mu(\varepsilon)}\left(1-\dfrac{\epsilon\varepsilon}{\epsilon_2}\right)\left(\dfrac{\epsilon_2}{|\epsilon_1|}\right)\left(\dfrac{\beta_2}{\beta_1}\right) \\ 0 \end{bmatrix} + \frac{2}{\mu(\varepsilon)} \begin{bmatrix} \beta_1\epsilon_1\left(1-\dfrac{\epsilon\varepsilon}{\epsilon_1}\right)v \\ -\beta_1\epsilon_1\left(1-\dfrac{\epsilon\varepsilon}{\epsilon_1}\right)u \\ \beta_2\epsilon_2\left(1-\dfrac{\epsilon\varepsilon}{\epsilon_2}\right)v \\ -\beta_2\epsilon_2\left(1-\dfrac{\epsilon\varepsilon}{\epsilon_2}\right)u \end{bmatrix} \qquad [2.18]$$

where

$$\bar{\beta}_j = \beta_j \frac{1+\epsilon_j}{1+\epsilon\varepsilon}\alpha_{jk}\frac{1}{\mu(\varepsilon)}, \quad A_{jk} = \frac{c_k}{\alpha_{jk}}. \qquad [2.19]$$

The last term in [2.18] reproduces the inertia modification of the centrifugal field, i.e. because of the u and v components the mixture is not in solid body rotation and the effective force-field differs from $\Omega^2 r\hat{r}$. This difference, however, can be shown to be relatively small when separation from solid body rotation is considered and $\epsilon\varepsilon$ is small. For this reason further progress can be made upon discarding the last term in [2.18].

Thus, we obtain a standard system for the calculation of u_{R1}, v_{R1}, u_{R2}, v_{R2} as functions of the variables ε_1 and ε_2 and the parameters ϵ_1, ϵ_2, β_1 and β_2.

We note that the procedure that led us from [2.9]–[2.10] to the present results can be straightforwardly extended to three and more components.

The insight gained by—and implementation of—[2.18] (with discarded last term) are enhanced by the following approximation. The coupling coefficients $\bar{\beta}_1 A_{12}$ and $\bar{\beta}_2 A_{21}$ are small in the range of interest which suggest that [2.18] can be rewritten as the limit $n \to \infty$ of the iterations

$$\begin{bmatrix} 1 & -2\bar{\beta}_1 \\ 2\bar{\beta}_1 & 1 \end{bmatrix} \begin{bmatrix} u_{R1}^{(n)} \\ v_{R1}^{(n)} \end{bmatrix} = \begin{bmatrix} \dfrac{r}{\mu(\varepsilon)}\left(1-\dfrac{\epsilon\varepsilon}{\epsilon_1}\right)\dfrac{\epsilon_1}{|\epsilon_1|} - 2\bar{\beta}_1 A_{12} v_{R2}^{(n-1)} \\ 2\bar{\beta}_1 A_{12} u_{R2}^{(n-1)} \end{bmatrix}$$

$$\begin{bmatrix} 1 & -2\bar{\beta}_2 \\ 2\bar{\beta}_2 & 1 \end{bmatrix} \begin{bmatrix} u_{R2}^{(n)} \\ v_{R2}^{(n)} \end{bmatrix} = \begin{bmatrix} \dfrac{r}{\mu(\varepsilon)}\left(1-\dfrac{\epsilon\varepsilon}{\epsilon_2}\right)\dfrac{\epsilon_2}{|\epsilon_1|}\left(\dfrac{\beta_2}{\beta_1}\right) - 2\bar{\beta}_2 A_{21} v_{R1}^{(n-1)} \\ 2\bar{\beta}_2 A_{21} u_{R1}^{(n-1)} \end{bmatrix}. \qquad [2.20]$$

We start with $n = 0$ and $u_{R_j}^{(-1)} = v_{R_j}^{(-1)} = 0$; this immediately yields

$$u_{Rj}^{(0)} = \frac{r}{\mu(\varepsilon)}\left(1-\frac{\epsilon\varepsilon}{\epsilon_j}\right)\frac{\epsilon_j}{|\epsilon_1|}\left(\frac{\beta_j}{\beta_1}\right)(1+4\bar{\beta}_j^2)^{-1}; \qquad [2.21a]$$

$$v_{Rj}^{(0)} = -2\bar{\beta}_j u_{Rj}^{(0)}. \qquad [2.21b]$$

The next, $n = 1$, iteration is straightforward. It can already be observed what is the effect of the coupling term: e.g. for $\epsilon_1 > 0$ and $\epsilon_2 > 0$ the positive initial radial velocity increases, and the negative azimuthal velocity also increases. In the cases reported below, accuracy better than 1% was obtained on the first, $n = 1$, iteration. The intermediate values in the iterations have, in general, no physical meaning. However, in the limiting case $\varepsilon_2 \to 0$, i.e. almost a monodispersion of particles

of type 1, (hence $A_{21}\to 0$) the exact values of u_{R1}, v_{R1} are already given by the $n=0$ iteration and the exact values of u_{R2}, v_{R2} by the next step.

From the theoretical point of view the Stokes drag and viscosity correlation [2.13] can be justified only in the limit $\beta_j\to 0$. However, to the best of our knowledge, there is no systematic information that can be used to replace [2.13] in a reliable manner for non-small β_j.

The asymptotic investigations of Childress (1964) and Herron *et al.* (1975) indicate that, for a single particle and $\beta_j \ll 1$,

$$\frac{\mathbf{d}_j}{\rho_C} = -\frac{9}{2}\frac{v_0}{a_j^2}\{\mathbf{v}_R + \sqrt{\beta_j}[A(u_R\hat{r} + v_R\hat{\theta}) + Cw_R\hat{z}] + \sqrt{\beta_j}B(-v_R\hat{r} + u_R\hat{\theta}) + O(\beta_j)\},$$

where $A = 15/7\sqrt{2}$, $B = 9/5\sqrt{2}$, $C = 12/7\sqrt{2}$. The corresponding relative velocity "postulate" (in the dilute limit $\varepsilon\to 0$) is

$$\mathbf{v}_{Rj} = \Omega r\epsilon_j\beta_j\left(1-\frac{\epsilon\varepsilon}{\epsilon_j}\right)\left[\frac{1+A\sqrt{\beta_j}}{1+2A\sqrt{\beta_j}} + O(\beta_j)\right]\left[\hat{r} - \frac{B\sqrt{\beta_j}}{1+A\sqrt{\beta_j}}\hat{\theta}\right]. \qquad [2.22]$$

Schaflinger *et al.* (1986) performed experiments with (monodispersed) suspensions of $0.07 < \beta < 5$ in a sectioned cylindrical centrifuge; the measured separation times compared favorably with predictions based on $\mathbf{v}_R$ obtained with [2.13], especially for $\beta \lesssim 1$. On the other hand, when [2.22] was used a big discrepancy resulted, see Ungarish (1993, section 7.5). This very restricted evidence seems to suggest that [2.18] is, practically, more recommended than [2.22] for $0 < \beta \lesssim 1$ although there is presently no theoretical explanation for this observation.

When $\beta_j \gg 1$ the flow field around the dispersed particle is certainly dominated by Coriolis effects which cause a special pressure distribution, so that the "form drag" becomes much more important than the possible viscous contribution [2.13]. For the "slow" lateral motion of a single particle in the limit $\beta_j\to\infty$, Stewartson's (1952) analysis predicts

$$\frac{\mathbf{d}_j}{\rho_C} = -2\pi\frac{1}{16+\pi^2}[(4u_R + \pi v_R)\hat{r} + (4v_R - \pi u_R)\hat{\theta}]. \qquad [2.23]$$

The corresponding relative velocity "postulate" can be obtained by substituting [2.23] in [2.11]–[2.12]. An indicative approximation is

$$\mathbf{v}_{Rj}^{(0)} = \Omega r\epsilon_j\left(1-\frac{\epsilon\varepsilon}{\epsilon_j}\right)(0.40\hat{r} - 0.49\hat{\theta}). \qquad [2.24]$$

To the best of our knowledge, there is no information on the practical applicability of the last result. The force [2.23] was obtained under the assumption that an infinitely long Taylor column is attached to the moving particle. This feature is evidently violated in a suspension where the typical distance between particles is of the order of their diameter. The relevant issues are yet at the stage of preliminary basic research (see Ungarish & Vedensky 1994, where also other important references are given).

An additional difficulty appears in the parametric range of non-small β: the averaged continuum mixture equations are not valid in the Ekman layers on the container's walls. [Note that the ratio of the Ekman thickness, $\sqrt{\nu_0/\Omega}$, to the particle radius, a, equals $(\sqrt{2}/3)\beta^{-\frac{1}{2}}$.]

Due to these difficulties and considerations we shall restrict our following discussion to small and moderately small β_j and use the "postulate" based on [2.13]. We bear in mind that the results must be subjected to experimental verifications.

3. SOLUTIONS

We consider the separation of a bi-dispersion in a straight axisymmetric cylinder. The suspension is initially in solid body rotation with the container and well-mixed, i.e.

$$u = v = w = 0, \quad \varepsilon_1 = \varepsilon_1(0), \quad \varepsilon_2 = \varepsilon_2(0) \quad \text{at } t = 0. \qquad [3.1]$$

For definiteness, unless stated otherwise, we shall focus attention on the case when both dispersed

phases are heavier than the fluid, i.e. $\epsilon_1 > 0$ and $\epsilon_2 > 0$. The analysis can be readily modified for cases when the dispersed phases are lighter than the fluid, or of opposed buoyancy-signs.

We use dimensionless variables, obtained by scaling the lengths with r_o, velocities with $|\epsilon_1|\beta_1\Omega r_o$ and the time with $1/|\epsilon_1|\beta_1\Omega$, cf. [2.17]; the scaling factors for the pressure and diffusion stress are $\rho_C|\epsilon_1|\beta_1(\Omega r_o)^2$ and $\rho_C(|\epsilon_1|\beta_1\Omega r_o)^2$, respectively.

3.1. Configuration 1: the infinite cylinder

When the axial length H is sufficiently large (as specified later) the influence of the "horizontal" walls $z = 0$ and $z = H$ can be neglected. The overall expected behavior of the separation process is similar to that in the gravity field, see figure 1.

Ungarish & Greenspan (1984) analyzed such a setup with $\epsilon_1 = \epsilon_2$ by employing the two-fluid model, but here we attempt the solution by the mixture model and do not restrict ourselves to $\epsilon_1 = \epsilon_2$.

The solution can be obtained by the following steps, see figure 1: treatment of the bidispersion sector (a); calculation of the motion and "jump conditions" on the interfaces (shocks) Σ_{ab} and Σ_S; analysis of the sediment layer; treatment of the mono-dispersion sector (b).

In the present infinite-cylinder axisymmetric geometry the solution is considerably facilitated by the fact that the flow field variables are independent of z and θ; consequently, the volume conservation $2\pi r\int_{z_1}^{z_2}\mathbf{j}\cdot\hat{r}dz = 0$ yields

$$\mathbf{j}\cdot\hat{r} = 0 \qquad [3.2]$$

at any point between the solid walls.

In sector (a), motivated by the monodispersed solution, we anticipate that the dependent variables are of the form

$$\varepsilon_j = \varepsilon_j(t); \quad p = \tfrac{1}{2}r^2\mathscr{P}(t); \qquad [3.3]$$

$$\mathbf{v}_f = rU_f(t)\hat{r} + r\omega_f(t)\hat{\theta} \quad \text{for } f = \mathrm{C},\ \mathrm{D}_j,\ \mathrm{R} \text{ or blank (mixture).} \qquad [3.4]$$

In view of [3.2] the radial component of the kinematic relationships [A12]–[A14] yield

$$U_C = -\sum_{j=1}^{2}\varepsilon_j U_{Rj}, \quad U_{Dj} = U_{Rj} - \sum_{j=1}^{2}\varepsilon_j U_{Rj},$$

$$U = \frac{1}{1+\epsilon\varepsilon}\sum_{j=1}^{2}(\epsilon_j - \epsilon\varepsilon)\varepsilon_j U_{Rj}. \qquad [3.5]$$

Now the continuity equations [2.7] read

$$\varepsilon_j' + 2\varepsilon_j U_{Dj} = 0, \quad j = 1, 2; \qquad [3.6]$$

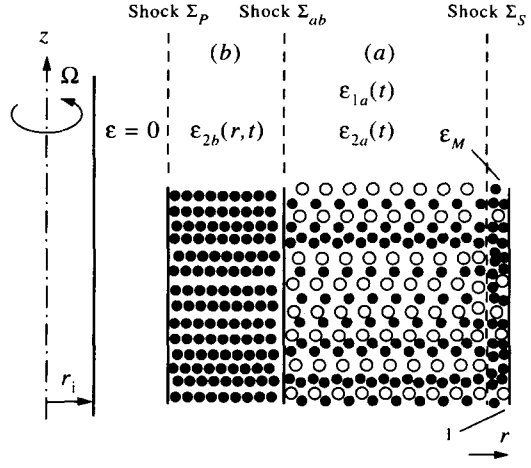

Figure 1. Sketch of infinite ("long") cylinder configuration.

which, on account of [3.5], can be expressed as

$$\varepsilon_1' + 2\varepsilon_1[(1-\varepsilon_1)U_{R1} - \varepsilon_2 U_{R2}] = 0; \tag{3.7}$$

$$\epsilon_2' + 2\varepsilon_2[(1-\varepsilon_2)U_{R2} - \varepsilon_1 U_{R1}] = 0; \tag{3.8}$$

the prime denotes the time derivative. We recall that the relative velocity $U_{Rj} = (u_{Rj}/r)$ has been "postulated" in the previous section. In particular, we can take [2.20], with $\varepsilon = \varepsilon_1(t) + \varepsilon_2(t)$. This combination yields an initial value system for the variables $\varepsilon_1(t)$, $\varepsilon_2(t)$, with starting values given by [3.1]. The numerical integration is straightforward.

If the $\varepsilon_j(t)$ and $U_{Rj}(t)$ are known the other radial velocities U, U_C and U_{Dj} are obtained by simple substitution in [3.5].

For further information on the flow field variables in sector (a) we must use the momentum balance [2.6]. Assuming that the generalized stress is Newtonian-like, the velocity field of the form [3.4] produces $\nabla \cdot \tau = 0$. After some arrangement we obtain:
the radial balance,

$$(1+\epsilon\varepsilon)[|\epsilon_1|\beta_1(U' + U^2 - \omega^2) - 2\omega] = -\mathscr{P} + \frac{\epsilon\varepsilon}{|\epsilon_1|\beta_1} + |\epsilon_1|\beta_1(\nabla \cdot \tau^{\text{diff}}) \cdot \hat{r}/r; \tag{3.9}$$

and the azimuthal momentum balance

$$(1+\epsilon\varepsilon)[|\epsilon_1|\beta_1(\omega' + 2U\omega) + 2U] = -4|\epsilon_1|\beta_1\left[\sum_{j=1}^{2}\left(1 - \frac{\varepsilon_j(1+\epsilon_j)}{1+\epsilon\varepsilon}\right)\varepsilon_j(1+\epsilon_j)U_{Rj}\omega_{Rj} - \varepsilon_1\varepsilon_2(1+\epsilon_1)(1+\epsilon_2)(U_{R1}\omega_{R2} + U_{R2}\omega_{R1})\right]. \tag{3.10}$$

It turns out that the radial momentum balance [3.9] is merely a definition of the pressure $\mathscr{P}(t)$; since this variable is not of major interest we did not calculate it. On the other hand, the azimuthal momentum balance [3.10] defines the angular velocity of the mixture, ω. We recall that U, U_{Rj}, ω_{Rj} and ε_j have been determined, hence the last equation can be easily numerically integrated, after a slight rearrangement, subject to the initial condition $\omega(t=0) = 0$. The cumbersome RHS of [3.10] is the contribution of the diffusion stress. This term actually turns out to be quite unimportant when $\beta_1 \ll 1$, in which case the Coriolis term $2U$ on the LHS dominates the behavior of $\omega(t)$.

We summarize: employing the "postulate" [2.20] for u_{Rj} and v_{Rj} the flow field variables in the bidispersed section (a) are obtained as a solution of a standard initial value system [3.7]–[3.8] and [3.10], supplemented by the relationships [3.5] and [3.9].

We note that the foregoing solution for the variables in the bidispersion sector (a) is "exact" in the sense that all the terms in the governing equations [2.5]–[2.7] have been incorporated. Approximations in the physical sense are evidently introduced by the "postulates" concerning τ and $\mathbf{v}_{Rj}$, and by the "long" cylinder idealization. We also note that initial conditions on $u = rU(t)$ cannot be applied. This indicates that some initial (presumably short) accommodation—or "relaxation"—process, not captured by the present formulation takes place, like in the monodispersed case (see Ungarish 1993, section 4.2).

Now we proceed to the calculation of the motion of the kinematic shocks Σ_{ab} and Σ_S. The radial velocity of the former is simply that of the fastest component in sector (a),

$$r'_{\Sigma_{ab}} = u_{\Sigma_{ab}} = r_{\Sigma_{ab}} U_{Dk}(t), \tag{3.11}$$

where $k = 1$ (usually) or 2 (for some combinations of parameters, see case C in examples below). Equation [3.11], subject to the initial condition $r_{\Sigma_{ab}} = r_i$, and in view of [3.6] yields

$$r_{\Sigma_{ab}}(t) = r_i\left(\frac{\varepsilon_k(0)}{\varepsilon_k(t)}\right)^{1/2}. \tag{3.12}$$

The radial velocity of the sediment shock Σ_S can be obtained from the assumption that the sediment is immobile (in the radial direction at least) and the volume fraction of the dispersed phase in this layer is the maximal packing fraction ε_M. Continuity of the dispersed phases over the

interface Σ_s then yields

$$\varepsilon_{ja}(u_{Dja} - u_{\Sigma_S}) = \varepsilon_{jS}(0 - u_{\Sigma_S}) \quad \text{for } j = 1, 2, \tag{3.13}$$

and

$$\varepsilon_{1S} + \varepsilon_{2S} = \varepsilon_M . \tag{3.14}$$

Since ε_{ja} and $u_{Dja} = rU_{Dj}$ have been determined, the calculation of ε_{jS} and of u_{Σ_S} is straightforward. In particular,

$$u_{\Sigma_S} = r'_{\Sigma_s} = -r_{\Sigma_s}(\varepsilon_{1a} U_{D1} + \varepsilon_{2a} U_{D2})/[\varepsilon_M - (\varepsilon_{1a} + \varepsilon_{2a})], \tag{3.15}$$

subject to the initial condition $r_{\Sigma_s}(0) = 1$. If $\alpha_M =$ constant as assumed here, and in view of [3.6], [3.15] can be integrated to the form

$$r_{\Sigma_S}(t) = \left(\frac{\varepsilon_M - [\varepsilon_1(0) + \varepsilon_2(0)]}{\varepsilon_M - [\varepsilon_{1a}(t) + \varepsilon_{2a}(t)]}\right)^{1/2}. \tag{3.16}$$

The thickness and structure of the sediment layer is evidently influenced by the choice of ε_M. The typical assumption for a sediment of monosized solid spheres, $\varepsilon_M =$ constant ≈ 0.65, must be reconsidered when the radii ratio a_2/a_1 is not close to 1. The possibility of smaller particles to fill the gaps between the larger ones renders a larger maximal packing fraction. If this ε_M is known in terms of a_2/a_1, ε_{1S}, ε_{2S} the solution of [3.13]–[3.15] can be modified accordingly, but a simple result like [3.16] no longer exists. Such effects on the bidispersed sediment in gravity separation have been investigated by Schneider *et al.* (1985), who employed a semi-empirical correlation for ε_M. The extension of that model to the present sediment layer is possible, but the applicability of that correlation to centrifugally-dominated packing requires investigations beyond the scope of this paper. We also note that the changes in ε_M may affect the effective viscosity function $\mu(\varepsilon)$ according to [2.13]. However, since $(1/\mu)\partial\mu/\partial\varepsilon_M \approx -1.25(\varepsilon/\varepsilon_M)^2 + O[(\varepsilon/\varepsilon_M)^3]$ this effect is small for $\varepsilon \leqslant 0.1$, say. In these cases the possible increase of ε_M may practically modify the details of the sediment layer, but not the solution in other domains.

Finally, we consider the sector (b) of monodispersed slower particles of type k left behind by the shock Σ_{ab}. The governing equations are

$$\mathbf{j} \cdot \hat{\mathbf{r}} = 0; \tag{3.17}$$

$$(1 + \epsilon\varepsilon)\left[|\epsilon_1|\beta_1\left(\frac{\partial u}{\partial t} + u\frac{\partial u}{\partial r} - \frac{v^2}{r}\right) - 2v\right] = -\frac{\mathrm{d}p}{\mathrm{d}r} + \frac{\epsilon}{\epsilon_1}\varepsilon r + E\mu(\varepsilon)(\nabla^2\mathbf{v}) \cdot \hat{r} + |\epsilon_1|\beta_1[\nabla \cdot \tau^{\mathrm{diff}}] \cdot \hat{r}; \tag{3.18}$$

$$(1 + \epsilon\varepsilon)\left[|\epsilon_1|\beta_1\left(\frac{\partial v}{\partial t} + u\frac{\partial v}{\partial r} + \frac{uv}{r}\right) + 2u\right] = E\mu(\varepsilon)(\nabla^2\mathbf{v}) \cdot \hat{\theta} + |\epsilon_1|\beta_1[\nabla \cdot \tau^{\mathrm{diff}}] \cdot \hat{\theta}; \tag{3.19}$$

$$\frac{\partial \varepsilon}{\partial t} + \frac{1}{r}\frac{\partial}{\partial r} r[\varepsilon(1 - \varepsilon)u_R + \varepsilon \mathbf{j} \cdot \hat{r}] = 0; \tag{3.20}$$

(since only one component is present, the appropriate subscript k is selfunderstood). Here

$$E = \nu_0/\Omega r_o^2$$

is the Ekman number.

The solution in sector (b) is complicated by the fact that the "initial" conditions are actually specified on the moving boundary $r = r_{\Sigma_{ab}}(t)$, via the "jump conditions" across the shock Σ_{ab}. Consequently, ε turns out to be a function of t and r, the velocities are not of the form [3.4] and the system [3.17]–[3.20] remains a genuine non-linear PDE one. This is in fundamental contrast with the (one-dimensional) gravity settling of a polydispersion where a simple structure is found in all the sectors.

The treatment of sector (b) is, however, facilitated by noticing that an "exact" solution for $\varepsilon(r, t)$ can be obtained as follows. The "postulate" for $\mathbf{v}_R$ presented in section 2.2 yields

$$u_R = rf_R(\varepsilon). \tag{3.21}$$

Table 1. Parameters in examples; in addition, $\varepsilon_M = 0.65$

Case	β_1	β_2	ϵ_1	ϵ_2	$\varepsilon_1(0)$	$\varepsilon_2(0)$
A	0.1	0.100	0.1	0.025	0.05	0.05
B	0.1	0.025	0.1	0.1	0.05	0.05
C	1.0	0.500	0.1	0.1	0.05	0.05
D	0.1	0.100	0.1	−0.1	0.05	0.05

In particular, for a single component, k, [2.20] produces

$$f_R(\varepsilon) = \frac{1-\varepsilon}{\mu(\varepsilon)} \frac{\epsilon_k}{|\epsilon_1|} \left(\frac{\beta_k}{\beta_1}\right) \left\{1 + 4\beta_k^2(1+\epsilon_k)^2 \left[\frac{1-\varepsilon}{(1+\varepsilon\epsilon_k)\mu(\varepsilon)}\right]^2\right\}^{-1}. \tag{3.22}$$

Hence [3.20], in view of [3.17] and [3.21], can be rewritten as

$$\frac{\partial \varepsilon}{\partial t} + r\left(\frac{\mathrm{d}}{\mathrm{d}\varepsilon}[\varepsilon(1-\varepsilon)f_R(\varepsilon)]\right)\frac{\partial \varepsilon}{\partial r} = -2\varepsilon(1-\varepsilon)f_R(\varepsilon). \tag{3.23}$$

This equation can be solved by the standard method of characteristics. Each characteristic line (denoted by the subscript ℓ) "starts" at the shock Σ_{ab} with

$$\varepsilon = \varepsilon_{kb} \quad \text{at} \quad t_\ell, \quad r = r_{\Sigma_{ab}}(t_\ell). \tag{3.24}$$

The value ε_{kb} is calculated from the continuity of the component k across the shock Σ_{ab},

$$\varepsilon_{kb}(u_{D_{kb}} - u_{\Sigma_{ab}}) = \varepsilon_{ka}(u_{Dka} - u_{\Sigma_{ab}}), \tag{3.25}$$

(again, the subscript k on the LHS is actually selfunderstood, because (b) is a monodispersed sector). This can be rewritten as

$$\varepsilon_{kb}[(1-\varepsilon_{kb})f_R(\varepsilon_{kb}) - U_{Dja}] = \varepsilon_{ka}(U_{Dka} - U_{Dja}), \tag{3.26}$$

where U_{Dja} is the reduced velocity of the fastest component in sector (a). Since the values in the RHS are known at any t_ℓ, [3.26] becomes a simple non-linear equation that defines $\varepsilon_{kb}(t_\ell)$. Starting with this value the numerical integration of [3.23]–[3.24] yields $\varepsilon[r, t; t_\ell)$ for $t \geqslant t_\ell$, $r_{\Sigma_{ab}}(t_\ell) \leqslant r < r_{\Sigma_{ab}}(t)$.

Next, the position of the mixture—pure fluid shock Σ_P can be calculated as the locus of the "last" particle that left the inner cylinder, i.e.

$$r'_{\Sigma_P} = u_{Dk} = r(1-\varepsilon)f_R(\varepsilon), \tag{3.27}$$

where [3.17], [3.21], [A.13] were used and, of course, the RHS is taken at $r = r_{\Sigma_P}(t)$ and $r_{\Sigma_P}(t=0) = r_i$, the inner radius.

The foregoing procedure provides ε, the radial velocities, v_R and r_{Σ_P} for the monodispersed sector (b) by quite straightforward calculation. If the pressure p and azimuthal velocity v are required, a more complicated numerical solution of the momentum equations [3.18]–[3.19] must be carried out.

We recall that in obtaining the approximation for $\mathbf{v}_R$ we discarded the last term of [2.18], in order to decouple between $\mathbf{v}_R$ and $\mathbf{v}$. Now it is possible to re-estimate the magnitude of the neglected terms and, if desired, to "correct" $\mathbf{v}_R$ and repeat the calculation of the flow-field variables with this improved value.

3.1.1. Examples. First, we performed comparisons with the "two-fluid" model results given in Ungarish & Greenspan (1984), and found excellent agreement. We note in passing that the velocity and time scalings differ by factor β_1 from the present values.

Here we present some additional results obtained for the combinations or parameters given in table 1. In all cases, the postulate [2.20] for $\mathbf{v}_R$ was used.

Some results are displayed in figures 2–4. For cases A, B and C we give details of ε_j, U_{Dj} and ω_{Rj} vs t in the bidispersed sector (a). For case A we also present ε_{jS} vs t in the sediment region adjacent to sector (a), the motion of the kinematic shocks and ε_2 vs r (for $r_i = 0.5$).

Cases A and B are quite similar, qualitatively and quantitatively, as regarding the separation process, i.e. the variables U_{Dj} and ε_j, as seen in figures 2(a), (b) and 3(a), (b). The particles of

component $j = 1$ are more buoyant in case A and larger in case B than of component $j = 2$, so that the ratios (ϵ_1/ϵ_2) in case A and β_1/β_2 (also, a_1^2/a_2^2) in case B are equal to 4. It is seen that the ratio U_{D1}/U_{D2} is, roughly, equal to this factor in both cases. This is in accordance with gravity settling knowledge.

The volume fraction of the more buoyant (larger) component $j = 1$ decays faster than that of the less buoyant (smaller) component $j = 2$, see figures 2(b) and 3(b). The "jump" of ε_2 from sector (a) to (b) on the shock Σ_{ab} is from a smaller to a larger value in both cases A and B. However, in the azimuthal component ω_{R2} there are differences between cases A and B as seen in figures 2(c) and 3(c), because this variable depends on the particular value of β_2, as indicated by [2.21b].

Figures 2(e) and (f) give information on the behavior of the left behind monodispersed sector (b) in a cylinder with inner radius $r_i = 0.5$. In this case the slower (in radial motion) component is $j = 2$. In this monodispersed sector the volume fraction decreases slightly with r. This radial "stratification", $\rho = [1 + \epsilon_2 \varepsilon(r, t)]\rho_C$, may be unstable in the centrifugal field, but this topic was not pursued here. Because of the abovementioned similarity between the radial motion in cases A and B, figures 2(e) and (f) are, roughly, also valid for the latter set in the same geometry.

Case C, with $\beta_1 = 1$ and $\beta_2 = 0.5$, is different from the previous ones in major features of the separation process as reflected by the behavior of the variables U_{Dj} and ε_j displayed in figures 4(a)

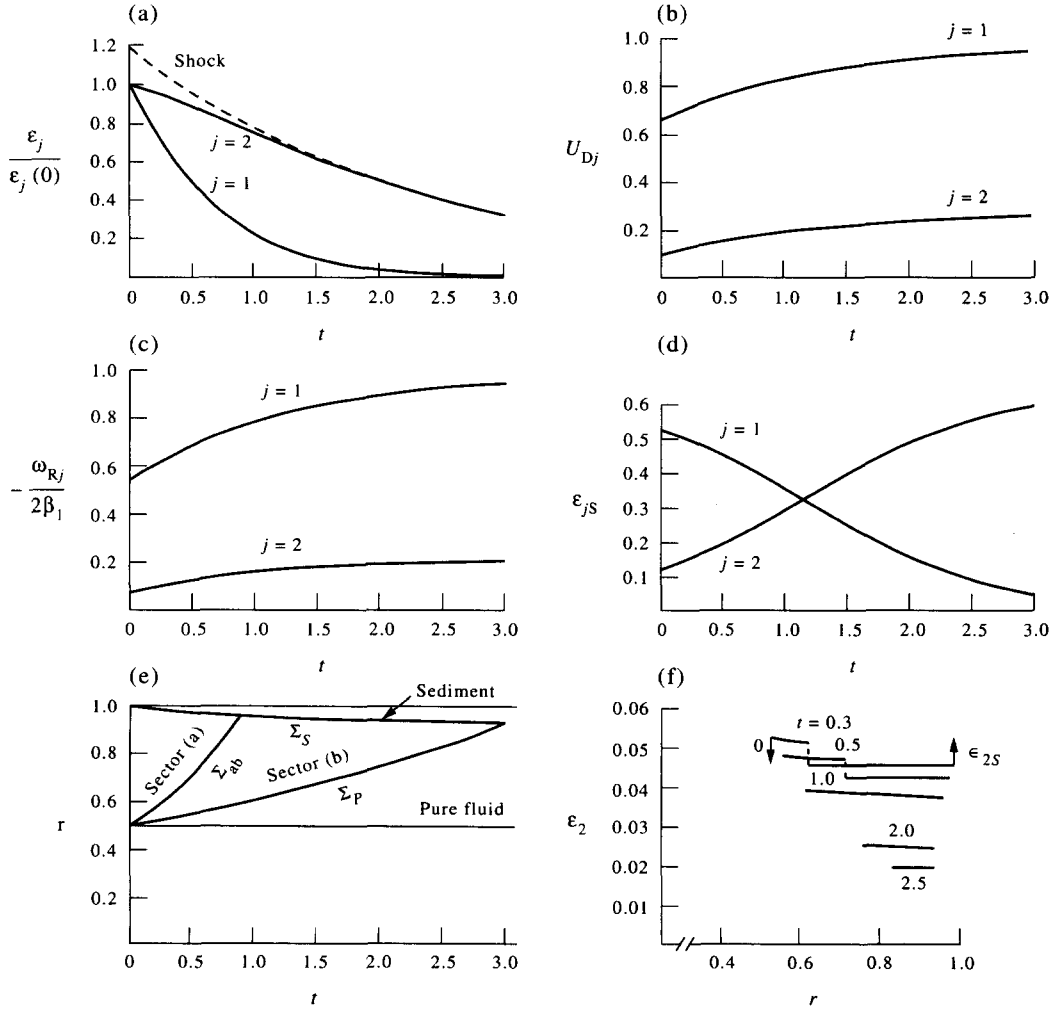

Figure 2. Long cylinder, case A: (a) $\varepsilon_j/\varepsilon_j(0)$ vs t, also $\varepsilon_{2b}/\varepsilon_2(0)$ on shock Σ_{ab} (---); (b) U_{Dj} vs t; (c) $-\omega_{Rj}/2\beta_1$ vs t; (d) ε_{jS} vs t; (e) sector diagram for $r_i = 0.5$; (f) ε_2 vs r at various t (the $\downarrow$ and $\uparrow$ indicate "jumps" to values 0 and ε_{2S}, respectively) for $r_i = 0.5$.

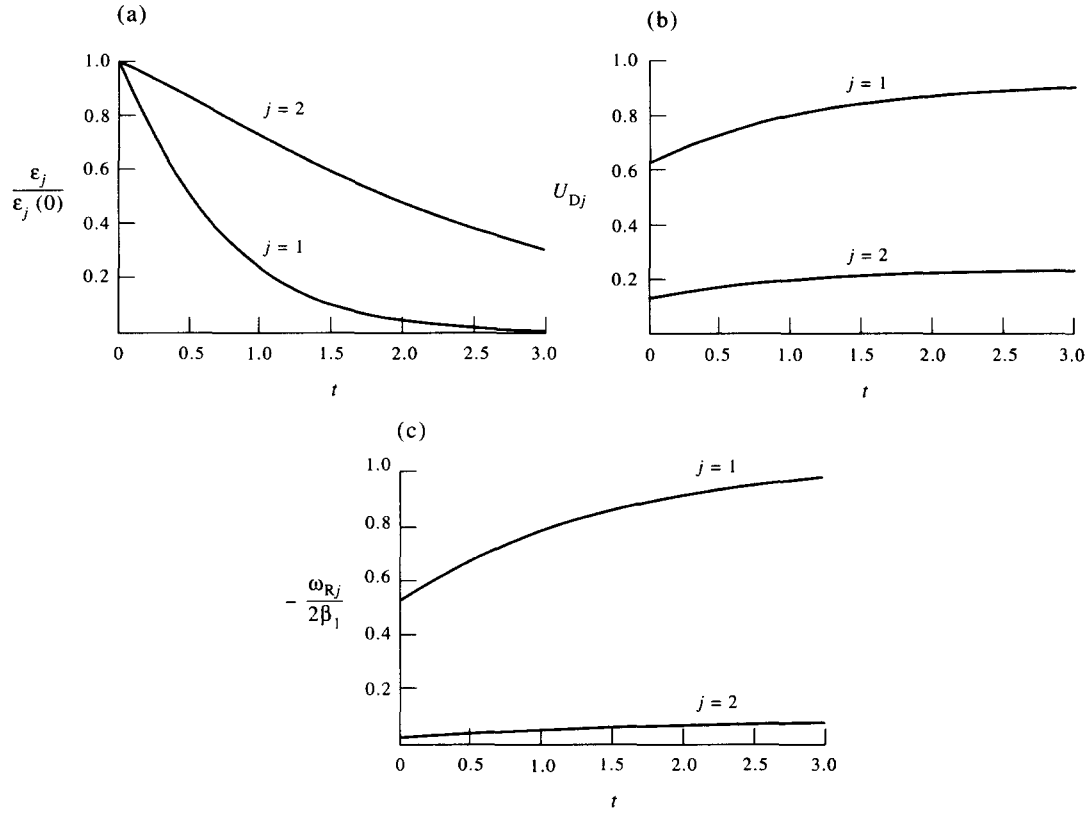

Figure 3. Long cylinder, case B: (a)–(c) as in figure 2.

and (b). The larger particles, $j = 1$, are slower and their volume fraction decays slower. In this case the component $j = 1$ is left behind in sector (b). The "jump" of ε_1 from sector (a) to (b) on the shock Σ_{ab} is from a larger to a smaller value. However, the azimuthal motion reflected by ω_{Rj} remains, qualitatively, like in cases A and B.

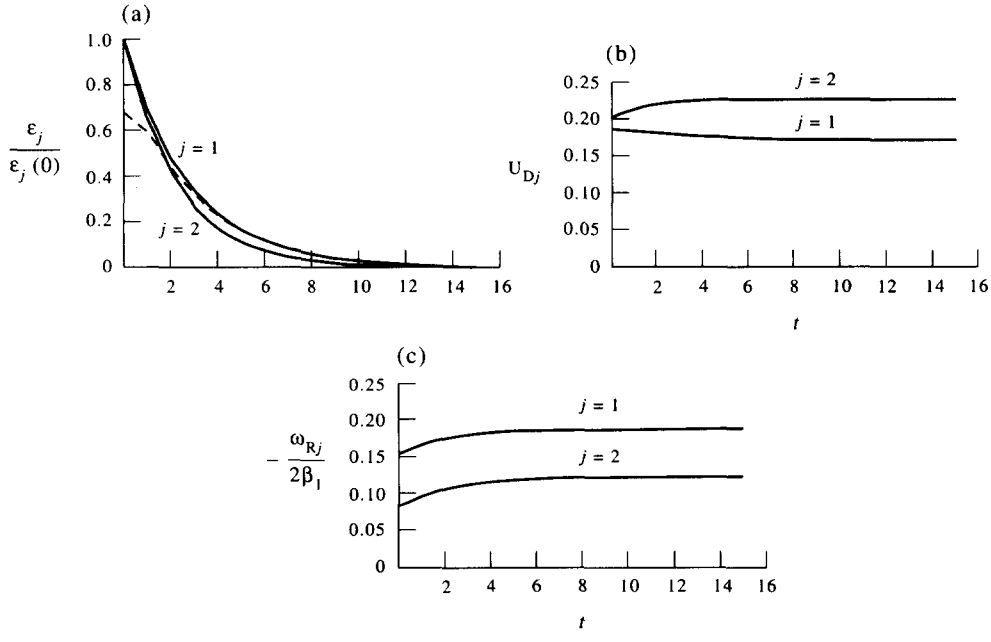

Figure 4. Long cylinder, case C: (a)–(c) as in figure 2.

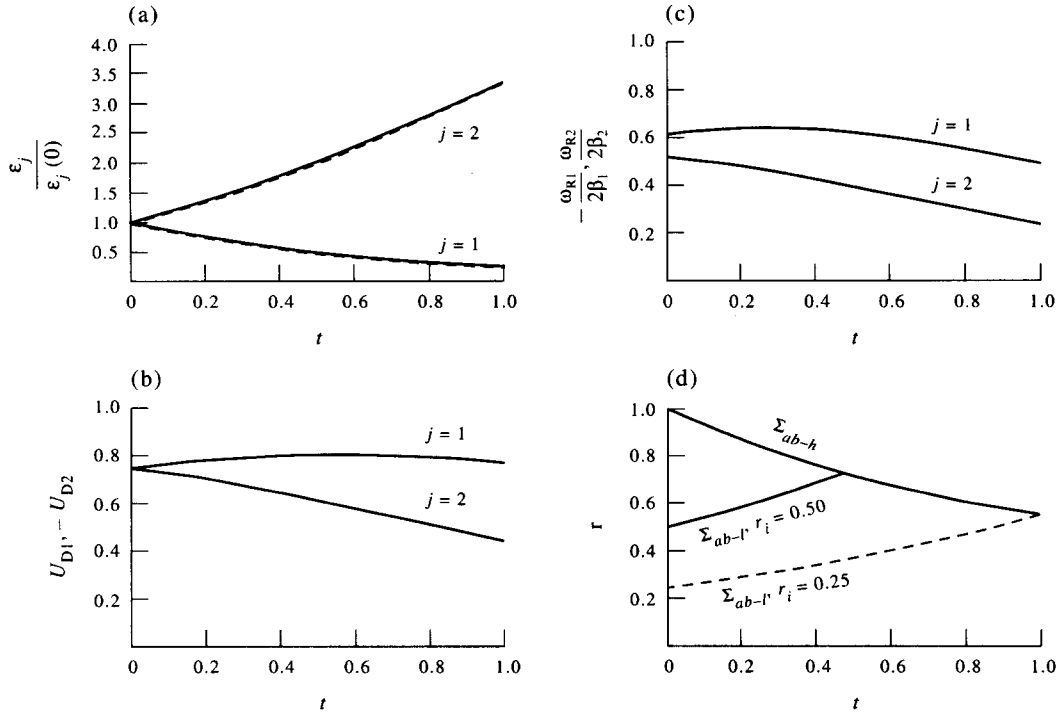

Figure 5. Long cylinder, case D: (a)–(c) as in figure 2; (d) motion of the shocks Σ_{ab-h} and Σ_{ab-l} that bound sector (a), the latter for cases with $r_i = 0.25$ and $r_i = 0.50$.

The conclusion is that for small values of β_j the main separative motion [i.e. propagation of the kinematic shocks Σ_S, Σ_{ab} and Σ_P and the profiles $\varepsilon_j(t)$] depends on the factors (ϵ_2/ϵ_1) and (β_2/β_1) in a similar manner. On the other hand, for $\beta_j > 0.5$ (say) some peculiar influences of the Coriolis acceleration show up and the dependency on (β_2/β_1) is not the same as before. In particular, larger particles may settle slower than the smaller ones, in which case sector (b) contains the larger particles, in contrast with gravity settling configurations. The same features for larger β_j were detected with the two-fluid model analysis by Ungarish & Greenspan (1984). The interpretation of this peculiar influence of β_j and its associated physical uncertainties are presented in Ungarish [1993, section 4.2.2]. Evidently, experimental verifications are necessary and it is our hope that the present methodology and solutions will stimulate conclusive experiments in this direction.

In case D the bidispersion contains both light and heavy particles. As shown in figure 5, the dispersed phases $j = 1$ and $j = 2$, with $\epsilon_1 = -\epsilon_2$, move in opposite directions with roughly equal velocities. Consequently, the sector (a) is embedded now in two monodispersed regions, (b – l) of the light particles and (b – h) of the heavy particles, with two corresponding kinematic shocks Σ_{ab-l} and Σ_{ab-h}, and contracts quickly (as compared to case A). In the bidispersed sector ε_1 decreases while ε_2 increases; the total ε increases.

In the gravity settling of heavy and light particles sector (a) is strongly unstable when $\varepsilon_1 + \varepsilon_2 = \varepsilon_1(0) + \varepsilon_2(0) > 0.16$ (typically), see Fessas & Weiland (1984). In the present centrifugal counterpart although $\varepsilon_1(0) + \varepsilon_2(0) = 0.1$ the critical value $\varepsilon = 0.16$ is, nevertheless, reached at $t \approx 1$. If the inner radius, r_i, is smaller than 0.25, separation of sector (a) is not completed yet at this time, and an interesting question is if the instability fingering shows up. Thus, the present results suggest an adequate experimental verification.

3.2. Configuration 2: the finite cylinder

Consider the system sketched in figure 6. It is known from the monodispersed analysis (see Ungarish 1993, section 5) that on the endplates $z = 0, H$ viscous shear layers of Ekman type appear. They influence mainly the azimuthal velocity, ω, during the separation process.

A corresponding investigation for a bidispersion is performed below. Comparing with the preceding infinite cylinder case, we must stress that now: (a) The facilitating condition $\mathbf{j} \cdot \hat{r} = 0$ is

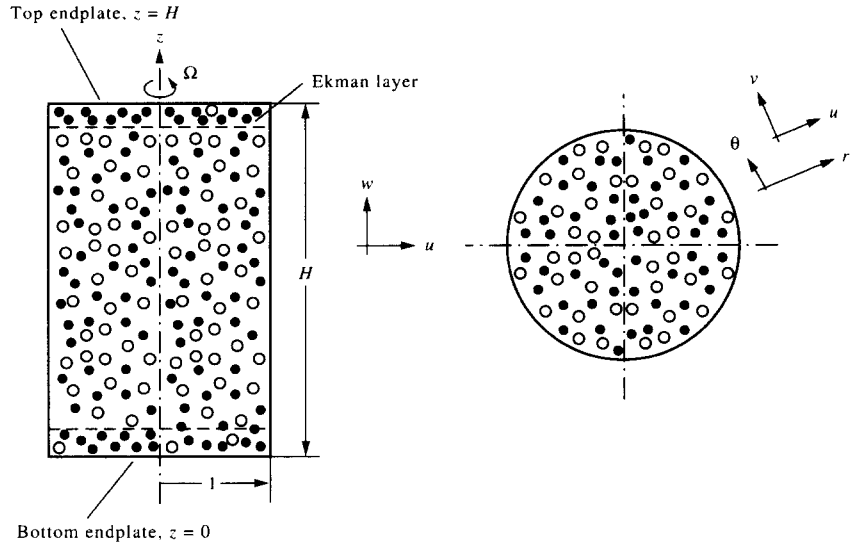

Figure 6. Sketch of finite cylinder configuration.

no longer valid, because the Ekman layers on the endplates introduce and support a radial volume transport, as seen below. (b) The analysis is restricted to $\beta_j \ll 1$; otherwise the thickness of the Ekman layer, $\sim(\nu_0/\Omega)^{1/2}$, cannot encompass many particles of diameter $2a_j$ and the averaged approach formulation becomes invalid in these critical shear layers.

An important parameter in this configuration is the Ekman number,

$$E = \frac{\nu_0}{\Omega r_o^2}, \tag{3.28}$$

assumed very small, as typical of practical centrifuges.

We separate the flow field into thin viscous Ekman layers (dimensionless thickness $\sim E^{1/2}$) and an inviscid "core" in the axial region $0^+ \leqslant z \leqslant H^-$. In the latter we anticipate

$$\varepsilon_j = \varepsilon_j(t); \quad p = \tfrac{1}{2}r^2\mathscr{P}(t) + E^{1/2}\frac{H}{4}\mathscr{L}(t)\left(\frac{2z}{H} - 1\right)^2; \tag{3.29}$$

$$\mathbf{v}_f = rU_f(t)\hat{r} + r\omega_f(t) + E^{1/2}W_f\left(\frac{2z}{H} - 1\right)\hat{z}; \tag{3.30}$$

for $f = \mathrm{C}, \mathrm{R}, \mathrm{D}j$ or blank. The axial velocity component, cf. [3.3]–[3.4], is introduced by the Ekman layer transport and is therefore assumed proportional to $E^{1/2}$. However, no axial separation effect is present so $W_\mathrm{R} = 0$ according to the postulate [2.18].

The governing equations [2.5]–[2.8] in the core region read now: global continuity,

$$\frac{1}{r}\frac{\partial}{\partial r}r(\mathbf{j}\cdot\hat{r}) + 2\frac{E^{1/2}}{H}W = 0; \tag{3.31}$$

global momentum balance,

(a) radial component given by [3.9];

(b) azimuthal component given by [3.10] which we repeat here,

$$(1+c\varepsilon)[|c_1|\beta_1(\omega' + 2U\omega) + 2U] = -4|c_1|\beta_1\left[\sum_{j=1}^{2}\left(1 - \frac{\varepsilon_j(1+c_j)}{1+c\varepsilon}\right)\varepsilon_j(1+c_j)U_{\mathrm{R}j}\omega_{\mathrm{R}j}\right.$$
$$\left. - \varepsilon_1\varepsilon_2(1+c_1)(1+c_2)(U_{\mathrm{R}1}\omega_{\mathrm{R}2} + U_{\mathrm{R}2}\omega_{\mathrm{R}1})\right]; \tag{3.32}$$

(c) axial component

$$(1+c\varepsilon)\left[|c_1|\beta_1 W' + E^{1/2}\frac{2}{H}W^2\right] = -\mathscr{L}; \tag{3.33}$$

dispersed phases continuity:

$$\varepsilon_1' + 2\varepsilon_1\left[(1-\varepsilon_1)U_{R1} - \varepsilon_2 U_{R2} + \frac{E^{1/2}}{H} W\right] = 0; \qquad [3.34]$$

$$\varepsilon_2' + 2\varepsilon_2\left[(1-\varepsilon_2)U_{R2} - \varepsilon_1 U_{R1} + \frac{E^{1/2}}{H} W\right] = 0. \qquad [3.35]$$

The matching of the foregoing "core" to the boundary conditions on the endplates via the Ekman layers produces the "Ekman suction" effect

$$w(z=0^+) = E^{1/2}\sqrt{\mu(\varepsilon)}\,\frac{1}{2}\frac{1}{r}\frac{\mathrm{d}}{\mathrm{d}r} rv(z=0^+), \qquad [3.36]$$

where $\mu(\varepsilon)$ was used to account for the effective viscosity in the shear region. In view of [3.30] we obtain from [3.36] the correlation

$$W(t) = -\sqrt{\mu[\varepsilon(t)]}\,\omega(t). \qquad [3.37]$$

This actually closes the system for the calculation of the variables in the core, for a given "postulate" for U_{Rj}, ω_{Rj}. To proceed, we integrate [3.31] and substitute [3.37] to obtain

$$\mathbf{j}\cdot\hat{r} = -\frac{E^{1/2}}{H} Wr = \frac{E^{1/2}}{H}\sqrt{\mu(\varepsilon)}\,\omega r. \qquad [3.38]$$

With this expression and the kinematic relationships [A.12]–[A.14] we can formally define U_{Dj}, U_C and U as functions of ε_j and ω; the results are similar to [3.5] plus the term [3.38]. In particular,

$$U = \frac{E^{1/2}}{H}\sqrt{\mu(\varepsilon)}\,\omega + \frac{1}{1+\epsilon\varepsilon}\sum_{j=1}^{2}(\epsilon_j - \epsilon\varepsilon)\varepsilon_j U_{Rj}. \qquad [3.39]$$

We observe that: (a) equations [3.34]–[3.35], [3.32], [3.37]–[3.39] form an independent standard initial value system for ε_j, U, ω and W; (b) the radial and axial momentum equations are merely definitions of the pressure functions $\mathscr{P}(t)$ and $\mathscr{L}(t)$.

The solution in the bidispersed core is, again, "exact"—like in the "long" cylinder configuration. Here the approximations are made in the Ekman suction correlation [3.37] and, again, in the postulate for $\mathbf{v}_R$.

Comparing [3.39] to [3.5] we conclude that the presence of the Ekman layer transport causes a decrease of the radial velocity U (ω is negative).

To gain additional insight on the influence of the endcaps let us consider the case $|\epsilon_j| \ll 1$ (and recall that also $\beta_j \ll 1$). The leading azimuthal momentum balance [3.32] can be approximated now by $|\epsilon_1|\beta_1\omega' + 2U = 0$, which, upon substitution of [3.39], can be expressed as

$$\omega' + 2\lambda_1\sqrt{\mu(\varepsilon)}\omega = -2\frac{1}{\beta_1}\sum_{j=1}^{2}\frac{\epsilon_j}{|\epsilon_1|}\left(1 - \frac{\epsilon\varepsilon}{\epsilon_j}\right)\varepsilon_j U_{Rj}, \qquad [3.40]$$

where

$$\lambda_1 = \frac{E^{1/2}}{|\epsilon_1|\beta_1 H}. \qquad [3.41]$$

The approximation [3.40] clearly shows that the Ekman layers have a major influence on the angular velocity of the mixture (in the rotating system). When λ_1 is not small ω is dampened by the viscous shear on the endplates, and the "long" cylinder case discussed in the foregoing section is recovered for $\lambda_1 \ll 1$.

In the monodispersion case the RHS of [3.40] equals $\beta^{-1}(\epsilon/|\epsilon|)\varepsilon'$, but here the connection between ω and ε is less explicit. As for orders of magnitude, we can estimate $\omega \sim \varepsilon(0)/\beta_1$ for small and moderate λ_1, and $\omega \sim \varepsilon(0)/\beta_1\lambda_1$ for large λ_1 (i.e. "strong" Ekman layers). With these outcomes, the relative contribution of the $(E^{1/2}/H)W$ terms in [3.34]–[3.35] is $O(\epsilon_1\lambda_1)$ for small and moderate λ_1 and $O(\epsilon_1)$ for large λ_1. This indicates that the Ekman layers have little influence on the behavior of $\varepsilon_j(t)$, i.e. the "long" cylinder solution for $\varepsilon_j(t)$ is a very good approximation for a finite cylinder. The calculations confirm this estimate.

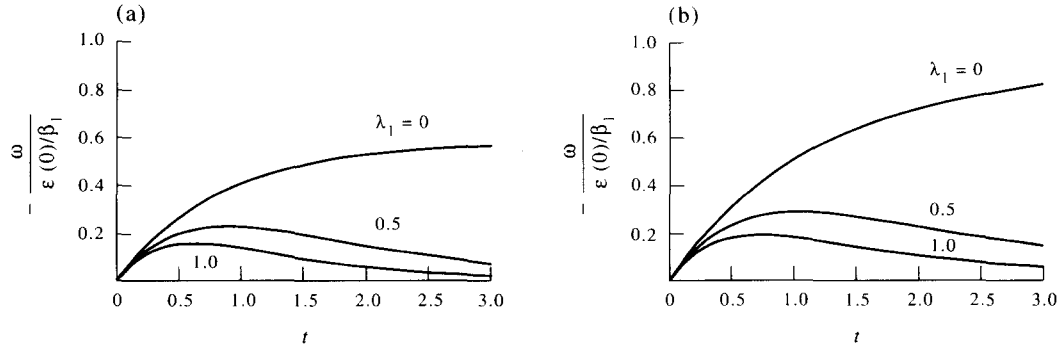

Figure 7. Finite cylinder, ω vs t, various λ_1: (a) case A; (b) case B.

3.2.1. Examples. We consider the influence of the endplates in cases A and B of table 1. The variables $\varepsilon_j(t)$, $U_{Dj}(t)$, $\omega_{Rj}(t)$ and $\omega(t)$ were calculated for $\lambda_1 = 0$, 0.5, 1, 2, 3 for $0 \leqslant t \leqslant 3$.

With the exception of $\omega(t)$, the dependency on λ_1 of these variables was found to be very weak, typically in the third significant digit.

On the other hand, the influence of λ_1 on the angular velocity of the mixture, $\omega(t)$, is pronounced, see figure 7. The result of the approximation [3.40] is compared with the "exact" result by [3.32] in figure 8 for case A and $\lambda_1 = 1$; the qualitative agreement is good, but the quantitative compatibility becomes poor after the peak of ω is reached. Similar behavior was noticed for other values of λ_1 and in case B. This confirms that basically ω in the core is induced by the separation between the phases and dampened by the Ekman layers, as seen in [3.40], and substantiates the relevance of the dimensionless parameter λ_1.

4. CONCLUDING REMARKS

The "mixture model" was extended for treatment of rotating polydispersed suspensions, and applications have been illustrated here for bidispersions in "long" and finite cylinders. It is expected that this model will enhance pertinent research in additional configurations, in order to close the gap of knowledge between gravity and centrifugal systems. Novel effects, with no counterpart in gravity settling, seem to be "hidden" in the range of non-small values of β and ε (say, $\beta_1 > 0.5$, $\varepsilon > 0.1$). Here, however, unsolved problems of drag and rheology make the analysis unreliable unless backed by stringent experiments.

For very small values of β_j the results are closer to the "intuition" provided by gravity settling and the model is more reliable. It is therefore anticipated that in this parametric range more centrifugal counterparts of known results in gravity polydispersed configurations will be soon confirmed and extended both analytically and experimentally.

Acknowledgment—This research was partially supported by the Fund for the Promotion of Research at the Technion.

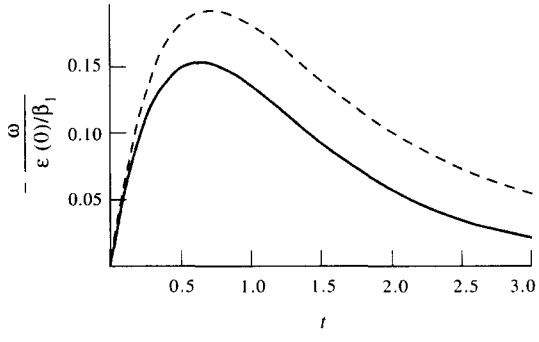

Figure 8. Finite cylinder, ω vs t, $\lambda_1 = 1$, "exact" and approximate (---) azimuthal equations.

REFERENCES

BATCHELOR, G. K. & VAN RENSBURG, R. W. J. 1986 Structure formation in bidisperse sedimentation. *J. Fluid Mech.* **166,** 379–407.

CHILDRESS, S. 1964 The slow motion of a sphere in a rotating, viscous fluid. *J. Fluid Mech.* **20,** 305–314.

DAVIS, R. H., HERBOLZHEIMER, E. & ACRIVOS, A. 1982 The sedimentation of polydisperse suspensions in vessels having inclined walls. *Int. J. Multiphase Flow* **8,** 571–585.

FESSAS, Y. P. & WEILAND, R. H. 1984 The settling of suspensions promoted by rigid buoyant particles. *Int. J. Multiphase Flow* **10,** 485–507.

GREENSPAN, H. P. & UNGARISH, M. 1982 On hindered settling of particles of different sizes. *Int. J. Multiphase Flow* **8,** 587–602.

HERRON, I. S., DAVIS, H. & BRETHERTON, F. P. 1975 On the sedimentation of a sphere in a centrifuge. *J. Fluid Mech.* **62,** 209–234.

HUPPERT, H. E., KERR, R. C., LISTER, J. R. & TURNER, J. S. 1991 Convection and particle entrainment driven by differential sedimentation. *J. Fluid Mech.* **226,** 349–369.

ISHII, M. & ZUBER, N. 1979 Drag coefficient and relative velocity in bubbly, droplet or particulate flow. *AIChE Jl* **25,** 843–854.

LAW, D. H.-S., MAC TAGGART, R. S., NANDAKUMAR, K. & MASLIYAH, J. H. 1988 Settling behavior of heavy and buoyant particles from a suspension in an inclined channel. *J. Fluid Mech.* **187,** 301–318.

SCHAFLINGER, U. 1985 Influence of nonuniform particle size on settling beneath downward facing inclined walls. *Int. J. Multiphase Flow* **11,** 783–796.

SCHAFLINGER, U., KÖPPL, A. & FILIPCZAK, G. 1986 Sedimentation in cylindrical centrifuges with compartments. *Ing. Arch.* **56,** 321–331.

SCHNEIDER, W., ANESTIS, G. & SCHLAFINGER, U. 1985 Sediment composition due to settling of particles of different sizes. *Int. J. Multiphase Flow* **11,** 419–423.

SMITH, T. N. 1966 The sedimentation of particles having a dispersion of sizes. *Trans. Inst. Chem. Engrs* **44,** 153–157.

STEWARTSON, K. 1952 On the slow motion of an ellipsoid in a rotating fluid. *Q. J. Mech. Appl. Math.* **6,** 141–162.

UNGARISH, M. 1995 Centrifugal separation of a polydispersed suspension in a long cylinder. *ZAMM 75 SI* 23–26.

UNGARISH, M. & GREENSPAN, H. P. 1984 On centrifugal separation of particles of two different sizes. *Int. J. Multiphase Flow* **10,** 133–148.

UNGARISH, M. 1993 *Hydrodynamics of suspensions: Fundamentals of Centrifugal and Gravity Separation.* Springer, Berlin.

UNGARISH M. & VEDENSKY, D. 1995 The motion of a rising disk in a rotating axially bounded fluid for large Taylor number. *J. Fluid Mech.* In press.

APPENDIX A

Some Kinematic Relationships

Define:

$$\varepsilon = \varepsilon_1 + \varepsilon_2; \tag{A1}$$

$$\epsilon_1 = (\rho_{D1} - \rho_C)/\rho_C; \quad \epsilon_2 = (\rho_{D2} - \rho_C)/\rho_C; \quad \epsilon = (\varepsilon_1\epsilon_1 + \varepsilon_2\epsilon_2)/\varepsilon; \tag{A2}$$

$$\rho = \varepsilon_1\rho_{D1} + \varepsilon_2\rho_{D2} + (1-\varepsilon)\rho_C; \tag{A3}$$

$$\mathbf{v}_{R1} = \mathbf{v}_{D1} - \mathbf{v}_C; \quad \mathbf{v}_{R2} = \mathbf{v}_{D2} - \mathbf{v}_C; \tag{A4}$$

$$\begin{aligned}\rho\mathbf{v} &= \rho_{D1}\varepsilon_1\mathbf{v}_{D1} + \rho_{D2}\varepsilon_2\mathbf{v}_{D2} + (1-\varepsilon)\rho_C\mathbf{v}_C \\ &= \rho\mathbf{v}_C + \varepsilon_1\rho_{D1}\mathbf{v}_{R1} + \varepsilon_2\rho_{D2}\mathbf{v}_{R2}.\end{aligned} \tag{A5}$$

Hence

$$\mathbf{v} = \mathbf{v}_C + \frac{1}{\rho}(\varepsilon_1\rho_{D1}\mathbf{v}_{R1} + \varepsilon_2\rho_{D2}\mathbf{v}_{R2}); \tag{A6}$$

$$\mathbf{v}_{Dj} = \mathbf{v} + \mathbf{v}_{Rj} - \frac{1}{\rho}\sum_{j=1}^{2} \varepsilon_j \rho_{Dj} \mathbf{v}_{Rj}. \tag{A7}$$

Using [A4] and [A5] we express

$$\rho_{D1}\mathbf{v}_{D1} - \rho\mathbf{v} = \rho_{D1}(\mathbf{v}_C + \mathbf{v}_{R1}) - \rho\mathbf{v} = \rho_{D1}\mathbf{v}_{R1} + \rho_{D1}\mathbf{v}_C - \rho\mathbf{v}, \tag{A8}$$

and eliminate $\mathbf{v}_C$ by [A6], rearrange and use [A2] to obtain

$$\frac{1}{\rho_C}[\rho_{D1}\mathbf{v}_{D1} - \rho\mathbf{v}] = \frac{1+\epsilon_1}{1+\epsilon\varepsilon}[(1-\varepsilon_1+\epsilon_2\varepsilon_2)\mathbf{v}_{R1} - \varepsilon_2(1+\epsilon_2)\mathbf{v}_{R2}] + (\epsilon_1 - \epsilon\varepsilon)\mathbf{v}. \tag{A9}$$

Similarly,

$$\frac{1}{\rho_C}[\rho_{D2}\mathbf{v}_{D2} - \rho\mathbf{v}] = \frac{1+\epsilon_2}{1+\epsilon\varepsilon}[(1-\varepsilon_2+\epsilon_1\varepsilon_1)\mathbf{v}_{R2} - \varepsilon_1(1+\epsilon_1)\mathbf{v}_{R1}] + (\epsilon_2 - \epsilon\varepsilon)\mathbf{v}. \tag{A10}$$

The volume flux is defined by

$$\mathbf{j} = \varepsilon_1 v_{D1} + \varepsilon_2 v_{D2} + (1-\varepsilon)v_C. \tag{A11}$$

Combining the last equation with [A1] and [A4] we get

$$\mathbf{v}_C = \mathbf{j} - \sum_{j=1}^{2} \varepsilon_j \mathbf{v}_{Rj}, \tag{A12}$$

and

$$\mathbf{v}_{Dj} = \mathbf{j} + \mathbf{v}_{Rj} - \sum_{j=1}^{2} \varepsilon_j \mathbf{v}_{Rj}. \tag{A13}$$

Combining [A12] and [A6] we obtain

$$\mathbf{v} = \mathbf{j} + \frac{1}{1+\epsilon\varepsilon}\sum_{j=1}^{2} (\epsilon_j - \epsilon\varepsilon)\varepsilon_j \mathbf{v}_{Rj}. \tag{A14}$$

APPENDIX B

The Diffusion Stress

The momentum flux in the bidispersion is

$$J = \sum_{j=1}^{2} \varepsilon_j \rho_{Dj} \mathbf{v}_{Dj}\mathbf{v}_{Dj} + (1-\varepsilon)\rho_C \mathbf{v}_C \mathbf{v}_C, \tag{B1}$$

and define

$$J = \rho\mathbf{v}\mathbf{v} - \tau^{\text{diff}}. \tag{B2}$$

Letting

$$\mathbf{w}_{Dj} = \mathbf{v}_{Dj} - \mathbf{v}, \quad \mathbf{w}_C = \mathbf{v}_C - \mathbf{v}, \tag{B3}$$

and substituting in [B1] we obtain, after some arrangements,

$$J = \rho\mathbf{v}\mathbf{v} + \left\{\sum_{j=1}^{2} \varepsilon_j \rho_{Dj}\mathbf{w}_{Dj}\mathbf{w}_{Dj} + (1-\varepsilon)\mathbf{w}_C\mathbf{w}_C\right\} + \mathbf{v}\mathbf{a} + \mathbf{a}\mathbf{v}, \tag{B4}$$

where

$$\mathbf{a} = \sum_{j=1}^{2} \varepsilon_j \rho_{Dj}\mathbf{w}_{Dj} + (1-\varepsilon)\rho_C\mathbf{w}_C = \sum_{j=1}^{2} \varepsilon_j \rho_{Dj}\mathbf{v}_{Dj} + (1-\varepsilon)\rho_C\mathbf{v}_C - \left[\sum_{j=1}^{2} \varepsilon_j \rho_{Dj} + (1-\varepsilon)\rho_C\right]\mathbf{v} = 0, \tag{B5}$$

recalling [A3]–[A5].

By [A6]–[A7]

$$\mathbf{w}_{Dj} = -\frac{1}{\rho}\sum_{j=1}^{2} \varepsilon_j \rho_{Dj}\mathbf{v}_{Rj} + \mathbf{v}_{Rj}, \quad \mathbf{w}_C = -\frac{1}{\rho}\sum_{j=1}^{2} \varepsilon_j \rho_{Dj}\mathbf{v}_{Rj}. \tag{B6}$$

Combining [B2]–[B6] we obtain [2.8].